Dual-color MINFLUX: Kinesin-1 takes Chassé-Inchworm steps

Lukas Scheiderer[1], Jan O. Wirth[1], Miroslaw Tarnawski[2], Stefan W. Hell[1,3*]

[1] Department of Optical Nanoscopy, Max Planck Institute for Medical Research, Heidelberg, Germany
[2] Protein Expression and Characterization Facility, Max Planck Institute for Medical Research, Heidelberg, Germany
[3] Department of NanoBiophotonics, Max Planck Institute for Multidisciplinary Sciences, Göttingen, Germany

*correspondence to shell@gwdg.de

Despite tremendous efforts using various techniques, many central questions regarding the walking mechanism of the ATP-driven motor protein kinesin-1 remained contradictory and puzzling. Still, it is widely believed that kinesin-1 walks hand-over-hand, meaning that the two motor domains (heads) sequentially overtake each other with a 16 nm step so that, after each step, the two heads are 8 nm apart. Here we developed dual-color fluorophore tracking by MINFLUX, which enabled us to follow the individual steps of the two heads simultaneously, up to physiological ATP concentrations. We found that, besides hand-over-hand, kinesin-1 frequently walks in a previously undescribed chassé-inchworm mode, whereby one of the heads advances by 16 nm, whereas the other one follows suit, binding in close proximity to the first. In this mode, the two heads are either 16 nm or ~0 nm apart. The transition between the two walking mechanisms is initiated by one of the heads making a large (>20 nm) passing step. MINFLUX also revealed that load-free kinesin-1 does not show significant limping and that the stalk folds back, pointing leftwards. The finding of the chassé-inchworm mechanism reconciles many of the contradictory results gained with other techniques, highlighting the power of multicolor MINFLUX tracking to reveal protein operation.

Kinesins form a superfamily of motor proteins that are essential for the directional transport of cargo along microtubules in cells[1]. Processive kinesins are mainly responsible for the transport of vesicles, synaptic vesicle precursors, lysosomes, organelles, protein complexes and neurofilament proteins towards the microtubular plus-end in the cell periphery[2]. They generally form homodimers consisting of two N-terminal motor domains (heads), two neck linkers, a stalk and a cargo-binding domain. The arguably best-studied member of the kinesin superfamily is kinesin-1 (here called kinesin for simplicity), a motor protein whose malfunction plays a role in many diseases.

Since its discovery in 1985[1], the walking of kinesin on microtubules has been studied with many techniques. Interference microscopy revealed that the motor consumes a single ATP molecule per 8 nm center-of-mass step[3]. Further insights have been gained by applying an inverted assay where the kinesin cargo site was immobilized onto a surface and the microtubule allowed to move in solution[4]. As the microtubules were found not to rotate but to progress in a single direction, it was concluded that kinesin advances linearly in an 'inchworm' or 'asymmetric hand-over-hand' fashion, without generating torque. The inchworm mechanism assumed a distinctly leading and trailing head, each making 8 nm steps so that the inter-head distances would alternate between 2 and 10 nm[4, 5]. The asymmetric hand-over-hand mechanism implied that kinesin walks like humans, with one of the heads on the right side of the stalk in walking direction and the other one on its left, so that no torque is generated. Symmetric hand-over-hand walking, on the other hand, meant that kinesin rotates around its stalk, like dancers, generating torque. Since no sign of microtubular rotation was found, the symmetric version was ruled out.

By succeeding in recording individual steps of a fluorophore-labeled head of single kinesin motors, the microscopy technique called FIONA subsequently tipped the balance towards the (asymmetric) hand-over-hand mechanism[5]. Concretely, it was found that a fluorophore linked to the front of a head takes steps of ~16 nm rather than the ~ 8 nm generally attributed to the inchworm. While FIONA could not establish whether the hand-over-hand walking was asymmetric or symmetric, combined with the inverted assay, the FIONA study appeared to vindicate the asymmetric (no-torque) version. In fact, animations of kinesin walking asymmetrically on microtubules like humans presently are among the best-known scientific cartoons.

Unfortunately, by relying on the detection of many thousand fluorescence photons on a camera, FIONA entails a prohibitively low spatio-temporal resolution of ~1 nm/ 330 ms. Therefore, FIONA was confined to studying kinesin slowed-down by ~100 times below physiological walking speed, accommodated by reducing the ATP concentration. Thus, FIONA may have missed out critical aspects of how kinesin walks at physiological ATP concentrations (1-5 mM).

Registering the bright light scattered from a large gold bead (diameter ≥30 nm) attached to one of the heads readily delivers the detected photon stream and hence the spatio-temporal resolution required for investigating normal kinesin walking with a camera. Two such studies revealed that the 16-nm steps actually consist of two successive ~8 nm substeps and that a moving head spends a few milliseconds in an unbound state before moving to its next binding site on the microtubule[6, 7]. Further advancements were made by tracking a 500 nm diameter bead attached to the stalk using an optical trap. Among others, the study using beads found that for certain kinesin constructs, the dwell times of the two heads on the microtubule differ significantly, amounting to substantial limping[8]. By contrast, other constructs showed similar dwell times of both heads, leaving the limping question unresolved and invoking the notion that the beads might have interfered with the actual kinesin walking.

Adding to the puzzle, a more recent optical trap study also found the generation of substantial torque under physiological ATP concentration[9], contradicting the conclusions drawn from the inverted-assay experiments. As the torque was unidirectional, these results could not be reconciled with a strict asymmetric hand-over-hand mechanism, leaving another conundrum in the quest for the real kinesin walking mechanism.

MINFLUX fluorophore tracking[10, 11] is a comparatively recent but promising addition to the toolbox for measuring conformational changes of proteins. By relying on direct labeling with a ~1 nm sized fluorophore, MINFLUX is minimally invasive like FIONA. However, by localizing with a beam featuring a central intensity minimum and a confocal detector, MINFLUX requires ~100 times fewer detected fluorescence photons per localization. The spatio-temporal resolution is thus improved to about ~1 nm / 5 ms. Being able to record kinesin stepping up to physiological ATP concentrations, MINFLUX readily detected the unbound substeps of the moving head, as well as its concomitant tendency to lean rightwards in the moving direction[12]. MINFLUX also detected a rotation of the stalk that accompanies stepping, consistent with the optical trap experiments displaying torque. Thus, it became clear that substantial progress can be made by developing a dual-color MINFLUX tracking system where two sites of the kinesin homodimer, such as both heads, or the head and the stalk, could be individually labeled and followed with minimal invasion and up to physiological walking speeds.

Results & Discussion

Our dual-color MINFLUX microscope (Fig. 1a) featured a green excitation beam (561 nm wavelength) paired with a 574-626 nm detection window for tracking the ‘green’ fluorophore Cy3B, as well as a red excitation beam (640 nm wavelength) paired with a 663-799 nm detection window for registering the ‘red’ fluorophore ATTO 643. Both excitation beams were optically designed to sequentially render a focal intensity distribution featuring a y- or x-oriented lined-shaped central intensity minimum in the

sample plane for MINFLUX localization in the x- or y-direction, respectively (Fig.1 a). The beams were applied in interlaced succession (Fig.1 b), so to allow localization of both fluorophores with ~5 nm precision within ~2 ms. Adjustment of the beams reduced the co-localization uncertainty ~1.5 nm.

We first tracked construct K28C (i.e., human kinesin with all surface-exposed cysteines replaced, truncated at amino acid position 560, C-terminal His6-tag). The heads were labeled with the fluorophores Cy3B and ATTO 643 via maleimide coupling. Complete labeling of all heads was confirmed by mass spectrometry. We recorded traces of kinesin walking on microtubules at 100 µM ATP concentration and displaying both colors. Averaging the measured positions between neighboring steps allowed to determine the step sizes with a precision of ~2 nm. By directly quantifying the distances between the two heads on the microtubular axis (x) we were able to observe whether the motor walked hand-over-hand, inchworm, or with another stepping mechanism.

Strikingly, we observed traces (Fig. 1c) where, in addition to a hand-over-hand mechanism, kinesin also displayed an inchworm-like walking. In the latter, one of the heads could be clearly identified as leading and the other one as trailing. The leading head leaps forward by 16 nm whereas the trailing head was pulled up to the leading head without overtaking it. Since the heads did not move in 8 nm steps as initially defined for the inchworm mechanism and no 2 or 10 nm residual distance could be established, we named the novel mechanism 'chassé-inchworm' (Fig. 1d). We also witnessed that kinesin shifted gears from chassé-inchworm to hand over hand Ⓐ and back Ⓑ (Fig.1c). Our interpretation (Fig.1f) is that the motor initially walks chassé-inchworm where the trailing head (red) takes a 16 nm step and reaches the binding site of the leading head (green) on the microtubule or one at a neighboring protofilament to the side. Next, the leading head (green) moves forward by 16 nm. After a large (> 20 nm) step Ⓐ of the head labeled with the red fluorophore, passing by its green-labeled counterpart, the motor clearly walks hand-over-hand, with the trailing head always overtaking the leading head so that the heads are ~8 nm apart each completed step. After a second large passing step Ⓑ of the red-labeled head, the latter stays in the lead and takes regular 16 nm steps with the green-labeled head approaching but never overtaking it.

This is a surprising finding. Although the majority of traces recorded at an ATP concentration of 100 µM seem to display the hand-over-hand mechanism (Fig.1 e) where the heads are separated by ~ ±8 nm, a fraction of traces display either exclusively the chassé-inchworm mechanism or a switch between the two mechanisms. To quantify the relative time spent in the two modes, we split the histogram (Fig. 1g) into five parts centered at the expected inter-fluorophore distances (-16 nm, -8 nm, 0 nm, 8 nm, 16 nm). Combining the percentages of -16 nm/0 nm/16 nm inter-fluorophore distances yielded an upper bound fraction of time spent in the chassé-inchworm mode of 43 % (the real value is only slightly lower as the fraction of substeps contributing to the 0 nm inter-fluorophore distance is negligible).

We also recorded dual-color (x, y) traces at a physiological 1 mM ATP concentration. An exemplary cutout (Fig. 2a) clearly displays interleaved steps of both heads spaced by ~8 nm, i.e., a hand-over-hand mechanism where the trailing head always passes its leading counterpart. By contrast, a clear chassé-inchworm stepping is displayed in another cutout (Fig.2b) where both heads are initially in close proximity. Subsequently, the green head takes a step of ~16 nm to the next binding site on its protofilament whereas the trailing head catches up and probably binds to an adjacent binding site, probably on a neighboring protofilament. While the hand-over-hand mechanism can be either asymmetric or symmetric, the chassé-inchworm mechanism is inherently asymmetric because one of the heads always leads while the other one trails. Therefore, most notably, the chassé-inchworm mechanism cannot generate torque.

Next, we recorded both heads again, in order to find out if kinesin limps. To rule out artefacts introduced by the position of the fluorophores, we additionally recorded traces of constructs T324C (Fig.3a) labeled

on the center right of the heads with respect to the walking direction and with the microtubule surface references as down. We also applied MINFLUX to construct E215C labeled in the front of the heads. The exemplary trace of T324C-Cy3B/ATTO 643 (Fig.3a) clearly shows chassé-inchworm stepping. Both heads take 16 nm steps but the red-labeled head never overtakes its green-labeled counterpart. The distance histogram (Fig.3b) clearly shows inter-fluorophore distances of mainly ~16 nm and ~0 nm. Calculating the time elapsed between successive steps of the heads allowed us to assess limping by establishing τ_1 and τ_2, denoting the time between step of the red head until completion of the step of the green head and vice versa, respectively. For example, the short exemplary trace (Fig.3a), happens to display a limp factor $L = \tau_1/\tau_2 \approx 2.55$ (Fig.3 c). To obtain a statistically more relevant limp factor of the load-free truncated kinesin, we combined the data from all constructs tracked at 100 µM ATP. Since each measurement was from a different kinesin molecule, we aimed to establish the highest possible limp factor as an upper bound. To this end, we determined for each trace which of both heads had the higher average τ_{high} and which had the lower average τ_{low}. The analysis of all traces showed that the average τ_{high} was not significantly higher than the average of τ_{low}, leading to a negligible upper bound $L \approx 1.29$ (Fig.3 d).

Splitting up the analysis revealed that for traces showing a clear chassé-inchworm mechanism, the L upper bound is ~1.67. However, for traces showing hand-over-hand movement the L upper bound is only ~1.34. This finding indicates that for hand-over-hand movement, the construct used exhibited no notable limping, which is expected when both heads are identical and move symmetrically. As for the chassé-inchworm mechanism, one might expect to see a difference in stepping kinetics between the two heads (Fig.3d, box plots). Yet in general, the upper bound of the limp factors were lower than the L ~1.8 simulated for a non-limping motor. Thus, for load-free constructs truncated at amino acid position 560 we can largely rule out substantial systematic limping.

To elucidate the orientation of the kinesin stalk during movement, we examined the position of the stalk in relation to one of the heads. The investigated construct featured a surface-exposed cysteine on the heads and two Halo-Tags at the stalk C-terminal. For most kinesins, both Halo-Tag moieties were labeled with the same type of fluorophore but only one of the two heads was labeled with the other fluorophore. Concretely, we recorded traces of the construct T324C-ATTO 647N-Halo-Cy3B with the head labeled with ATTO 647N and the stalk with Cy3B (Fig.4a). The histogram of distances between the fluorophores along the longitudinal microtubule axis (Fig.4b) revealed that the distribution is rather broad and centered at ~ 0 nm. Hence, for this cargo-free construct, the stalk does not specifically extend backwards during stepping.

When analyzing the off-axis histogram (Fig.4c), it is important to bear in mind that the cylindrical microtubules are three-dimensional whereas our MINFLUX system tracks only in the focal plane (x,y). Hence, we see only projections of movements into the central x,y- plane of the microtubules. These projections depend on whether the motor walks on top of the microtubule or on its left or right side in walking direction. For example, if the stalk was pointing upwards within the reference system of a kinesin walking on the microtubule side, the measured displacement would be sideways in the coordinate system of the microscope. Since the motors should walk on the left and right side with equal probability, one would expect a similar occurrence of leftward and rightward apparent displacements of the stalk.

However, the histogram of measured off-axis distances, based on 68 traces, is clearly asymmetric, peaking at around 10 nm. This result implies that the fluorophore on the stalk is displaced to the left from the labeled position on the head. This finding is actually in agreement with the T324C-Halo dimer structure predicted by AlphaFold (Fig.4d). Interestingly, Alphafold also predicted a second structure with a folded-back stalk entailing an inter-fluorophore spacing of ~20 nm. This possible structure suggests that the flexible stalk could also accommodate a more elongated conformation, which is in line with the up to ~20 nm inter-fluorophore displacements also found in the histogram.

We note that the negative values in the histogram could, in principle, also arise from motors walking on the bottom of the microtubule, but this scenario is virtually excluded by the fact that the bottom half of the microtubule is blocked by the coverslip and microtubule-immobilizing agents. Since the majority of traces are expected to come from motors walking on the top half, the asymmetry in the histogram should be due to the actual orientation of the cargo-free stalk. Combining the results from the on-axis and off-axis histograms allowed us to conclude that the ~40 nm long stalk is folded back, pointing to the left in walking direction (Fig.4d).

Altogether, by tracking two sites of homodimeric kinesin simultaneously with minimally invasive labels at up to physiological ATP concentrations, dual-color MINFLUX clearly advances the understanding of kinesin walking. Yet, the most striking finding is that the motor protein can draw on (at least) two radically different walking mechanisms: a chassé-inchworm mechanism that is inherently asymmetric and does not generate torque, and a head-over-head mechanism that can be either asymmetric or symmetric, with only the latter producing torque. Single-color MINFLUX tracking recently showed that kinesin stepping is biased to the right, in support of the symmetric movement[12]. Moreover, compelling evidence from optical trap experiments showed that kinesin produces torque[9], in stark contrast to the arresting inverted assay experiments[4] showing that no torque is generated. Our discovery that kinesin can walk in two distinct ways clearly offers a reconciling explanation: the hand-over-hand mechanism is symmetric producing torque, whereas in the chassé-inchworm phase the production of torque is absent. In the inverted assay, kinesin may have resorted to the chassé-inchworm mode, possibly because the torque required for rotating a lengthy microtubule in a viscous solution may have been too large. While the quickly improving capabilities of MINFLUX will certainly shed further light on (motor) protein function, our current understanding is that kinesin walks with equal efficiency both in a (symmetric, torque-generating) hand-over hand and an asymmetric torque-free chassé-inchworm manner (Movie1), depending on interactions and circumstances that are yet to be discovered.

Author Contributions: L.S. designed and performed the kinesin measurements, evaluated and interpreted data, with initial input from J.O.W. and S.W.H.. L.S. scrutinized the kinesin-1 literature on walking mechanisms and limping. J.O.W. built and characterized the performance of the dual-color MINFLUX microscope, and wrote the evaluation software. M.T. produced the kinesin-1 constructs. Developing MINFLUX tracking, S.W.H. initiated the dual-color study and was responsible for supervision, steering and, along with L.S. and J.O.W., for critical interpretation of the findings. L.S. and S.W.H. wrote the paper with input from all authors.

Acknowledgements: We acknowledge our colleagues Alexey Butkevich for the synthesis of halo-Cy3B, Johann Engelhardt for contributions to the development of the MINFLUX system utilize and Steffen Sahl for critical reading. We thank Ahmet Yildiz for providing kinesin plasmid K560CLM T324C and Ron Vale for providing kinesin plasmid K560CLM E215C.

Competing interests: S.W.H. has revenues through patents on MINFLUX held by the Max Planck Society and through shares of Abberior Instruments GmbH. All other authors declare no competing interests.

Funding: No external funding.

References

1. Vale, R.D., T.S. Reese, and M.P. Sheetz, *Identification of a novel force-generating protein, kinesin, involved in microtubule-based motility.* Cell, 1985. **42**(1): p. 39-50.
2. Vale, R.D. and R.A. Milligan, *The way things move: Looking under the hood of molecular motor proteins.* Science, 2000. **288**(5463): p. 88-95.
3. Schnitzer, M.J. and S.M. Block, *Kinesin hydrolyses one ATP per 8-nm step.* Nature, 1997. **388**(6640): p. 386-390.
4. Hua, W., J. Chung, and J. Gelles, *Distinguishing inchworm and hand-over-hand processive kinesin movement by neck rotation measurements.* Science, 2002. **295**(5556): p. 844-848.
5. Yildiz, A., et al., *Kinesin walks hand-over-hand.* Science, 2004. **303**(5658): p. 676-678.
6. Mickolajczyk, K.J., et al., *Kinetics of nucleotide-dependent structural transitions in the kinesin-1 hydrolysis cycle.* Proceedings of the National Academy of Sciences of the United States of America, 2015. **112**(52): p. E7186-E7193.
7. Isojima, H., et al., *Direct observation of intermediate states during the stepping motion of kinesin-1.* Nature Chemical Biology, 2016. **12**(4): p. 290-+.
8. Asbury, C.L., A.N. Fehr, and S.M. Block, *Kinesin moves by an asymmetric hand-over-hand mechanism.* Science, 2003. **302**(5653): p. 2130-4.
9. Ramaiya, A., et al., *Kinesin rotates unidirectionally and generates torque while walking on microtubules.* Proceedings of the National Academy of Sciences of the United States of America, 2017. **114**(41): p. 10894-10899.
10. Balzarotti, F., et al., *Nanometer resolution imaging and tracking of fluorescent molecules with minimal photon fluxes.* Science, 2017. **355**(6325): p. 606-612.
11. Eilers, Y., et al., *MINFLUX monitors rapid molecular jumps with superior spatiotemporal resolution.* Proceedings of the National Academy of Sciences of the United States of America, 2018. **115**(24): p. 6117-6122.
12. Wirth, J.O., et al., *MINFLUX dissects the unimpeded walking of kinesin-1.* Science, 2023. **379**(6636): p. 1004-1010.

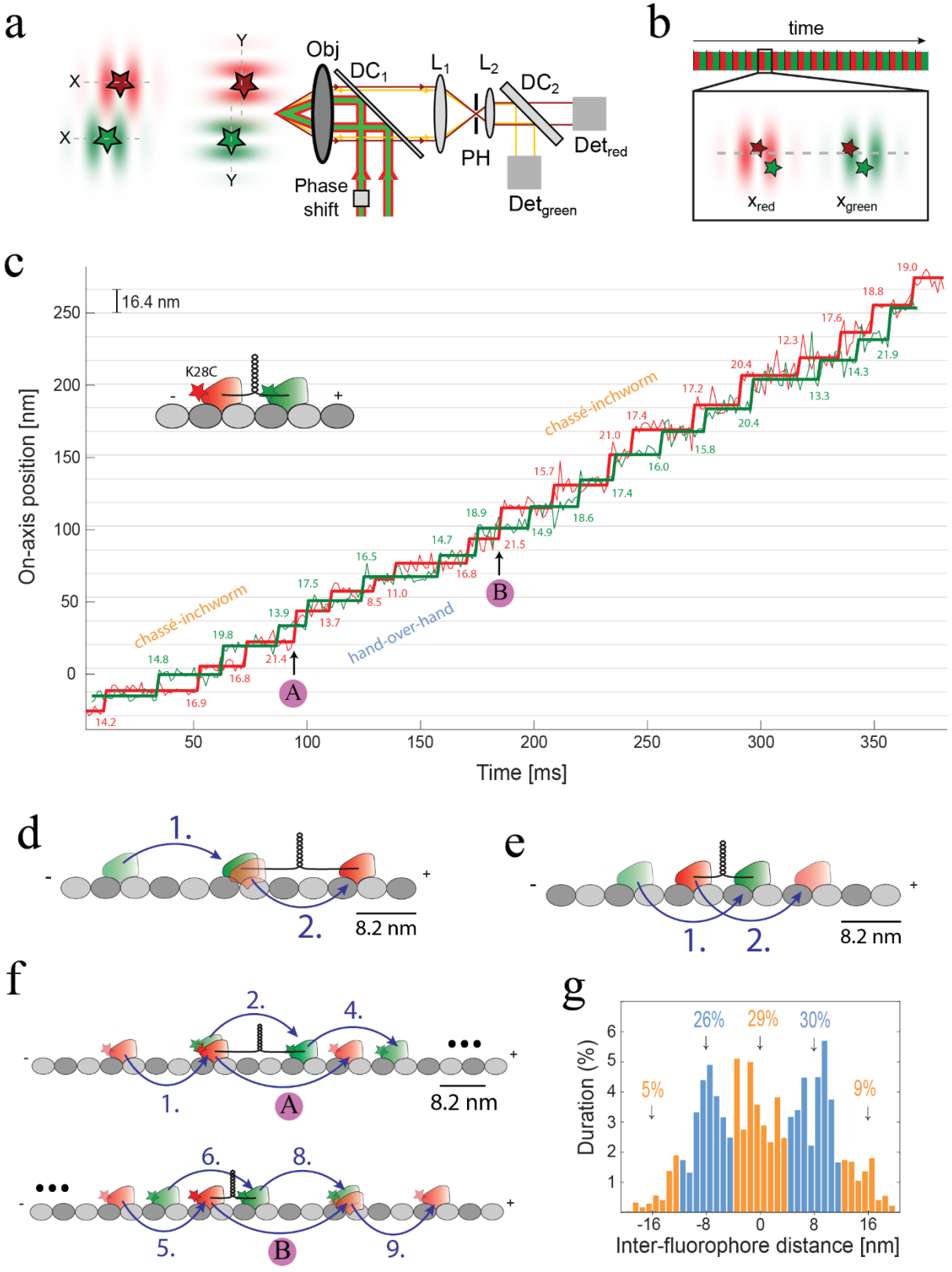

Fig. 1: Dual-color MINFLUX fluorophore tracking reveals that kinesin switches between phases of hand-over-hand and chassé-inchworm walking. **a**, MINFLUX localization of a green and a red fluorophore (stars) is accomplished with x- and y-oriented focal excitation intensity distributions having line-shaped central intensity minima created by destructive interference (using phase shifter PS) of green and of red excitation light around the focal point of the objective lens (Obj). Here sketched with a spatial offset for clarity, the green and red beams are perfectly overlaid at the sample. Dichroic mirror DC_1 separates excitation from fluorescence light, and after

passing lens L_1, the confocal pinhole PH and lens L_2, the fluorescence is split by DC_2 so that the light emitted by the green and the red fluorophore is detected by Det_{green} and Det_{red}, respectively. **b**, Dual-color recording and localization is implemented in a time-interlaced mode, with each localization lasting ~2 ms. **c,** One-dimensional trace of labeled kinesin construct K28C-Cy3B/ATTO 643 displaying the fluorophore position along the microtubule axis over time along with the fitted step function. Kinesin exhibits first a chassé-inchworm movement, with the green-labeled head in the lead, a switch to hand-over-hand at Ⓐ and a second switch at Ⓑ to chassé-inchworm mode, with the red head in the lead. **d,** Basic chassé-inchworm step with distinctly leading and trailing heads, **e**, Basic hand-over hand mechanism with the trailing head always passing the leading head. **f,** Switching mechanisms: after two chassé-inchworm steps (1.,2.), the trailing red head takes a large passing step (Ⓐ) and the motor continues hand-over-hand. After the second passing step (Ⓑ), the motor walks chassé-inchworm again (8.,9.), but with the red head in the lead. Cy3B: green star; ATTO 643: red star. **g**, Histogram of inter-fluorophore distance durations of traces from three constructs (K28C, E215C, T324C) at 100 µM ATP. Percentages of each segment are indicated. Bars in blue: hand-over-hand; bars in orange: chassé-inchworm.

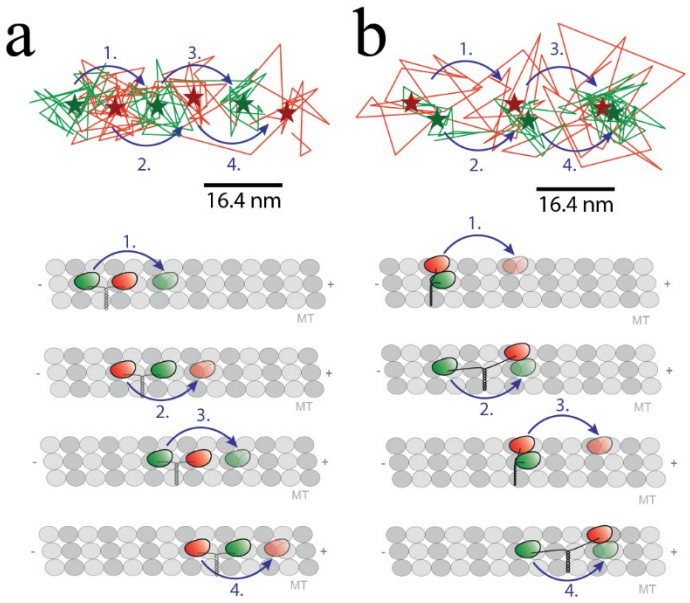

Fig. 2: Comparison of hand-over-hand and chassé mechanisms using sections of exemplary two-dimensional (2D) traces of K28C-Cy3B/ATTO 643 at physiological 1 mM ATP concentration. **a,** (top) trace displaying steps and (below) sketched interpretation as hand-over-hand mechanism walking on the microtubule (grey). **b**, analogous to **a**, but for chassé-inchworm mechanism. The stars mark the fitted interstep plateaus.

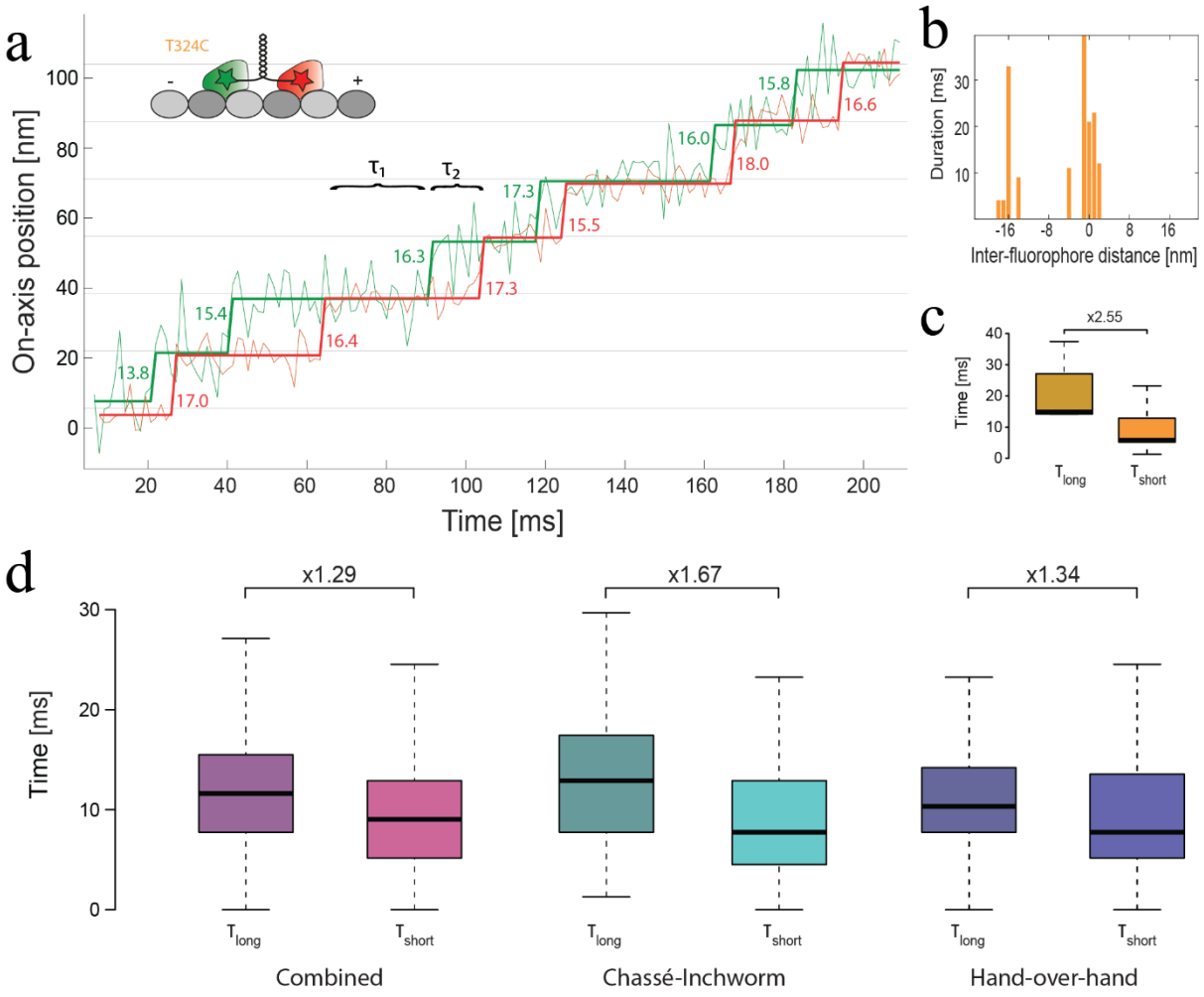

Fig. 3: Limping evaluation of kinesin-1. **a**, Exemplary dual-color 1D trace of kinesin-1 construct T324C-Cy3B/ATTO 643 (cartoon inset) walking chassé-inchworm along the microtubule axis and fitted step function. Examples of the interstep dwell times τ_1 (red head step until green head step) and τ_2 (green head step until red head step) are indicated with brackets. **b**, Inter-fluorophore distance histogram of the exemplary trace, featuring two peaks at -16 nm and 0 nm, indicative of chassé-inchworm walking. **c**, Box plot of all τ_1 and τ_2 from the exemplary trace, yielding a limping factor $L = \tilde{\tau_1}/\tilde{\tau_2}$ of 2.55 from the median interstep times. **d**, Box plots of the longer (τ_{long}) and shorter (τ_{short}) interstep times of traces from the three constructs (K28C, E215C, T324C) at an ATP concentration of 100 µM. For each trace, the interstep times τ_1 and τ_2 are assigned. The respective interstep times with the higher mean are added to the distribution of τ_{long} and the respective interstep times with the lower mean are added to the distribution of τ_{short}. The magenta boxes are plotted from all traces, the cyan boxes from a subset of traces displaying exclusively a chassé-inchworm mechanism and the green traces from a subset of traces displaying exclusively a hand-over-hand mechanism.

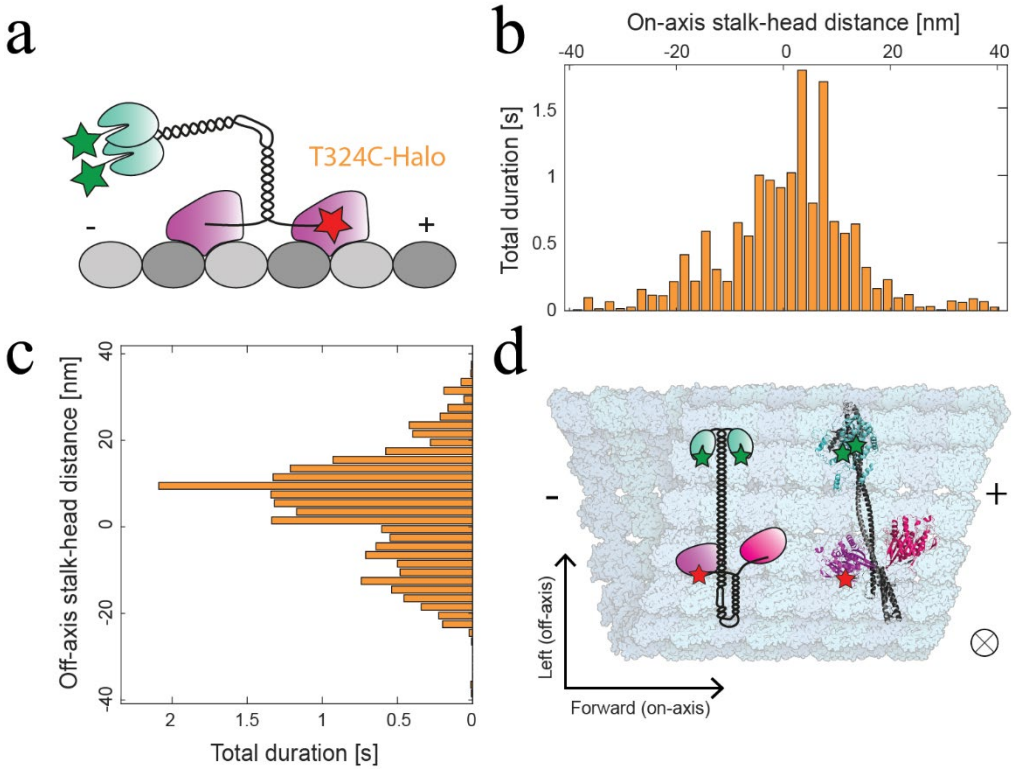

Fig. 4: Reconstruction of the stalk orientation of cargo-free kinesin-1. **a**, Cartoon of the labeled stalk-head construct T324C-ATTO 647N-Halo-Cy3B. **b**, Histogram of on-axis inter-fluorophore distance along the microtubule axis. **c**, Histogram of off-axis inter-fluorophore distance orthogonal to the microtubule axis revealing the stalk to be displaced from the motor domain by ~10 nm to the left most of the time. **d**, Reconstructed orientation of the stalk-head construct on a microtubule. The cartoon on the left showing the motor domain (magenta), the folded-back stalk (black) and the Halotag fused C-terminally to the stalk (cyan). The protein structure predicted by Alphafold on the right (green) displays a folded-back stalk with a calculated inter-fluorophore spacing of ~10 nm. The symbol ⊗ is pointing downwards towards the coverslip and microscope objective.